



## An System Based On STM32 And Piezoresistive Air Pressure Sensor

---

Xiangmin Hu

EasyChair preprints are intended for rapid dissemination of research results and are integrated with the rest of EasyChair.

August 5, 2020

# An System Based On STM32 And Piezoresistive Air Pressure Sensor

HU Xiangmin  
Robotics Academy  
Guangdong Polytechnic Of Science And Technology  
Zhuhai , China  
e-mail: hxm126@hotmail.com

**Abstract**—Breath pressure is a very common measurement parameter of health intelligent products. In this paper, piezoresistive bridge air pressure sensor is used as data acquisition component. Using precision instrument amplifier and adjusting circuit amplifier as signal processing unit , STM32F103c8t6 control system is data processing unit. Optimize the circuit design of instrument amplifier, Overcome the weak signal and the temperature drift error and nonlinear error, Complete the hardware system design of respiratory pressure detection, amplification, control and display system.

**Keywords:** Piezoresistive bridge; Sensor; Instrument amplifier; STM32

## I. INTRODUCTION

With the progress of science and technology and the improvement of living standards, people pay more and more attention to health. Intelligent health electronic products are emerging. There is also an increasing number of analog signals for human health monitoring. These simulated signals include blood oxygen, blood pressure, breathing pressure, etc. All kinds of human health and exercise data are future health products testing objectives. Respiratory pressure as a very important and typical simulation monitoring volume is very important representative and universal. The accuracy of the breathing pressure measurement directly affects the subsequent control and judgment. At the same time, sensors are also evolving to intelligent, miniaturized, and various MEMS devices are developing rapidly. The piezoelectric effect transforms the pressure signal into an electrical signal. Pressure-resisting pressure sensors have many advantages in process manufacturing, cost, sensitivity and long-term stability. As a classic structure of pressure-resisting sensors, Wheatstone bridge has a common application scenario. In this paper, STM32F103C8T6 is selected as the control core of the data acquisition system, completes the processing, control and display of data, selects NXP's pressure sensor MPXC201DT1 to collect air pressure data, and AD623 instrumentation amplifier as differential amplifier. The key to the design of data acquisition system is to overcome the common mode error of weak signal, bias voltage, bias current and various noise in the operation and operation circuit. The optimal design and performance research of the air pressure detection circuit around the instrument amplifier is very necessary and is also the key to the whole data acquisition system.

## II. HARDWARE SYSTEM DESIGN

### A. Overall Structure of Hardware System

The STM32F103C8T6 is a 32-bit Microprocessor based on the ARM Cortex-M core STM32 series, with a program memory capacity of 64KB, a voltage of 2V-3.6V, and a operating temperature of -40C-85C. According to the system functional requirements, the function block diagram of the air pressure data acquisition system is shown in Figure 1:

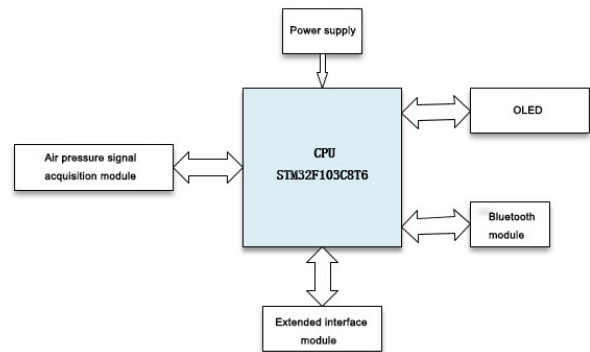


Figure 1. System function block diagram

### B. Air Pressure Sensor Data Acquisition System Design

Because the data collected by the sensor itself is in millivolt level, and the various sources of error from the outside world have a greater impact on the measurement results. Therefore, eliminating the error of current and the current noise of the amplifier itself is the key to the design of the data acquisition system.

The inside of the instrumentation amplifier itself is current-driven and rear-protected. The AD623 is a low-cost, high-precision instrumentation amplifier that requires only one external resistor to set the gain, with a gain range of 1 to 10000. The AD623 is available in an 8-pin SOIC and DIP package, smaller than discrete circuit designs and has lower power consumption (maximum operating current of only 1.3mA), making it ideal for battery-powered and portable applications. The AD623 is ideal for precision data acquisition systems such as scales and sensor interfaces with high accuracy (maximum non-linearity of 40ppm), low offset voltage and low offset drift. In addition, the AD623 has low noise, low input bias currents and low power consumption, making it ideal for medical applications such

as ECG and non-invasive blood pressure monitors. In this paper, a single-supply-powered AD623 is selected as the *amplification unit* of system data acquisition. The overall design of the system is shown in Figure 2.

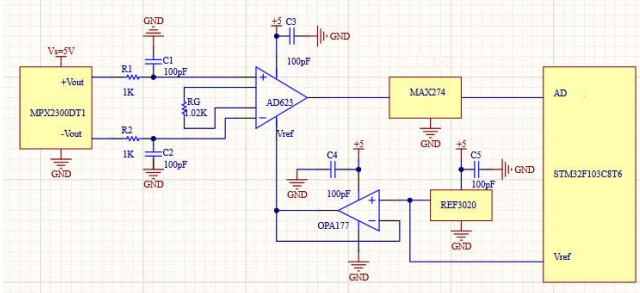


Figure 2. Overall system design

- In this data pressure data acquisition system, the pressure sensor uses NXP's pressure-resisting sensor MPX2300DT1. The sensor has a certain price advantage, it self-contained Wheatstone bridge and temperature compensation and calibration circuit, to complete the acquisition of weak air pressure signal.
- The design is optimized around the instrument amplifier AD623 to reduce the various noise and bias voltage currents of the circuit.

First, the common mode suppression ratio (CMRR) of the instrument amplifier itself alone is not sufficient to provide robust noise suppression in harsh industrial use environments, and to avoid the propagation of excess noise signals, it is essential to properly match and adjust the components in the instrument input low-pass filter. Ultimately, internal electromagnetic interference/radio frequency interference (EMI/RFI) filtering and CMRR work together to reduce other noise to achieve an acceptable signal-to-noise ratio (SNR). Amplification of pressure sensors or temperature sensor signals is a common application of instrumentation amplifiers. Due to the RF rectifier inside the instrument amplifier itself, there is a strong RF interference until the offset affecting the DC output voltage, and the most practical way to solve this type of problem is to use differential low pass filter as the RF attenuation filter at the front of the instrument amplifier. This circuit designs a balanced RC low-pass filter circuit at the front end of the AD623 to do attenuation.

Second, a simple RC low-pass anti-aliasing filter is usually used between the output of the instrumentation amplifier and the input of the ADC to reduce off-band noise. If the reference input pin of the instrumentation amplifier is connected directly to a simple divider, the symmetry of the subtractor circuit and the voltage divider ratio are changed. It also reduces the common mode suppression ratio of the instrumentation amplifier and its gain accuracy. This circuit provides a low-power op amp buffer OPA177 between the voltage divider and the instrumentation amplifier reference input. The op amp buffer acts as an active filter, which allows the use of capacitors with much smaller capacitances to decouple to the same large power supply. In addition, active filters can be used to increase the Q value to speed up

the on-time, eliminate the problem of impedance matching and temperature coefficient matching, and make it easy to adjust the reference voltage. The single-supply op amp circuit requires a bias common mode input voltage amplitude to control the forward and negative swings of the AC signal. When the bias voltage is provided using the divider from the supply voltage, proper decoupling is required to ensure the performance of the PSR. C3, C4, C5 and other decoupling capacitors are designed in the circuit.

Finally, between the AD input pins of the AD623 and THE STM32F103, the Max274, creates a low-pass filter to further attenuate the high-frequency noise generated by the circuit. Using the REF3020 standard regulator chip to provide a stable 2.048V reference voltage, the voltage reference end Vref provided to SMT32F103, to provide reference voltage for AD conversion. At the same time, the reference voltage is provided for the OPA177. According to the parameters of the pressure sensor MPX2300DT1, the 6V reference voltage outputs the measured voltage of 3.006MV at full scale. If the voltage is 5V output at full-scale, the voltage is approximately 2.5MV. The AD623 has a magnification of 100 and a full-scale measurement of approximately 2.298V, based on a reference voltage of 2.048V, to meet the measurement requirements.

### C. Power Supply Module Design

The entire system operates at 5V and 3.3V voltage conditions, the USB interface provides 5V power supply, the LM1117MP for steady voltage output of 3.3V voltage, providing the system put most of the 5V voltage and 3.3V supply voltage of 32-bit processor.

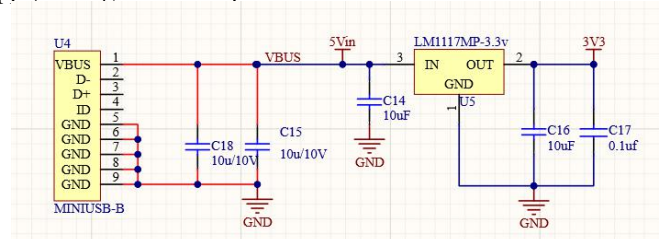


Figure 3. Power supply

### D. Display Module Design

The display module is 0.96 inch OLED module, which is connected to the SMT32F103C8T6 via the I2C interface. The interface design of the display interface to the ARM processor is shown in Figure 4.

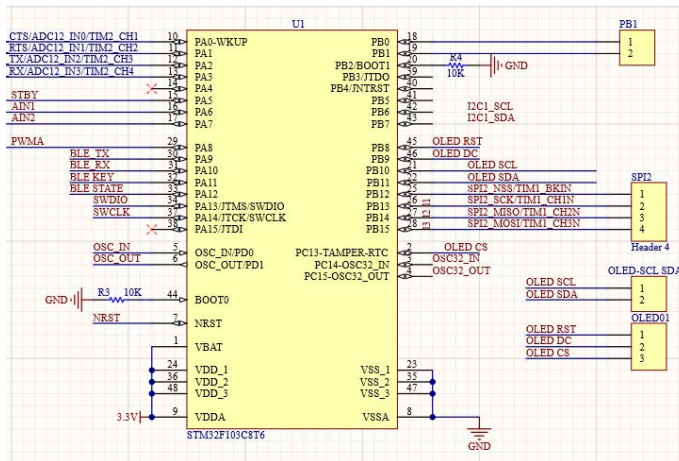


Figure 4. OLED display interface circuit

### E. Bluetooth Module Design

Data acquisition terminal sized with a dedicated HC05 Bluetooth module to realize the data interaction with other terminals in local networking and mobile phone APP.

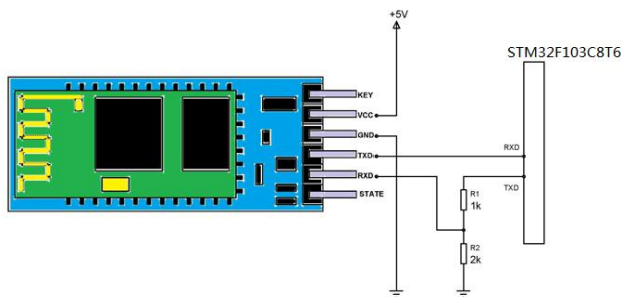


Figure 5. Bluetooth module

## III. CONCLUSIONS

The system design is based on the Control Core of SMT32F103C8T6, uses the NXP pressure sensor MPX2300DT1 for data acquisition, optimizes the design around the single-supply instrument amendumeter amplifier AD623, and completes the design of the system hardware system. Measurement accuracy meets the technical requirements of general health equipment and consumes low power.

## REFERENCES

- [1] Zhong,X.Y,Wang, Y.P, Liao,C.R. Liu, S.Tang, J.Wang, Q. Temperature-insensitivity gas pressure sensor based on inflated long period fiber grating inscribed in photonic crystal fiber. Opt. Lett. 2015, 40, 1791-1794.
- [2] Tang, J.Zhang, Z.Yin, G. Liu, S.Bai, Z.Li, Z.Deng, M.Wang, Y.Liao, C.He, J. et al. Long period fibergrating inscribed in hollow-core photonic bandgap fiber for gas pressure sensing. IEEE Photonics J. 2017, 9,1-7.
- [3] Huang, B.Ying, W.Mao, C. Wang, Y. Temperature-and strain-insensitive transverse load sensing based on optical fiber reflective Lyot filter. Appl. Phys. Express 2019, 12, 076501.

- [4] H. Goto, Y. Hasegawa, and M. Tanaka, "Efficient Scheduling Focusing on the Duality of MPL Representatives," Proc. ASME Symp. Computational IntelligenceLiu, Q.; Li, S.G.; Chen, H. Enhanced sensitivity of temperature sensor by a PCF with a defect core based on Sagnac interferometer. Sens. Actuators B 2018, 254, 636-641.
- [5] Ma, J.; Jin, W.; Ho, H.L.; Dai, J.Y. High-sensitivity fiber-tip pressure sensor with graphene diaphragm.Opt. Lett. 2012, 37, 2493-2495.
- [6] Kachuee, M.; Kiani, M.M.; Mohammadzade, H.; Shabany, M. Cuffless blood pressure estimation algorithms for continuous health-care monitoring. IEEE Trans. Biomed. Eng. 2017, 64, 859-869.
- [7] I. F. Akyildiz and I. H. Kasimoglu, "Wireless sensor and actor networks: research challenges," Ad Hoc Networks, vol. 2, no. 4, pp. 351-367, 2004.
- [8] C. C. Lin, R. G. Lee, and C. C. Hsiao, "A pervasive health monitoring service system based on ubiquitous network technology," International Journal of Medical Informatics, vol. 77, no. 7, pp. 461-469, 2008.
- [9] Y. J. Chang and W. T. Huang, "A novel design of data-driven architecture for remote monitoring and remote control of sensors over a wireless sensor network and the Internet," Journal of Internet Technology, vol. 12, no. 1, pp. 129-138,2011.
- [10] Suo, J.; Yao, Z.; Zhang, B.; Li, C. Charger mobility scheduling and modeling in wireless rechargeable sensor networks. In Proceedings of the International Wireless Communications and Mobile Computing Conference,Cyprus, Paphos, 5-9 September 2016.
- [11] Silvani, X.; Morandini, F.; Innocenti, E.; Peres, S. Evaluation of a wireless sensor network with low cost and low energy consumption for fire detection and monitoring. Fire Technol. 2015, 51, 971-993.
- [12] Beata, P.; Jeffers, A.; Kamat, V. Real-time fire monitoring and visualization for the post-ignition fire state in a building. Fire Technol. 2018, 1-33.
- [13] Martins, M.S.; Correia, V.; Lanceros-Mendez, S.; Cabral, J.M.; Rocha, J.G. Comparative finite element analyses of piezoelectric ceramics and polymers at high frequency for underwater wireless communications.Procedia Eng. 2010, 5, 99-102.
- [14] Xu, Q.C.; Yoshikawa, S.; Belsick, J.R.; Newnham, R.E. Piezoelectric Composites with High Sensitivity and High Capacitance for Use at High Pressures. IEEE Trans. Ultrason. Ferroelectr. Freq. Control 1991, 38, 634-638.
- [15] Ausanio, G.; Barone, A.C.; Hison, C.; Iannotti, V.; Mannara, G.; Lanotte, L. Magnetoelastic sensor application in civil buildings monitoring. Sens. Actuators A 2005, 123/124, 290-295.
- [16] Kaniusas, E.; Pftzner, H.; Mehnen, L.; Kosel, J. Magnetoelastic skin curvature sensor for biomedical applications. In Proceedings of the IEEE Sensors, Vienna, Austria, 24-27 October 2004; pp. 1484-1487.
- [17] Pongponsri, S.; Yu, X.H. An adaptive filtering approach for electrocardiogram (ECG) signal noise reduction using neural networks. Neurocomputing 2013, 117, 206-213.
- [18] Schlegelmilch, F.; Schellhorn, K.; Stein, P. A method for online correction of artifacts in EEG signals during transcranial electrical stimulation. Clin. Neurophysiol. 2013, 124, e166-e168.
- [19] Leahy, R.; Mosher, J.; Spencer, M.; Huang, M.; Lewine, J. A study of dipole localization accuracy for MEG and EEG using a human skull phantom. Electroencephal. Clin. Neurophysiol. 1998, 107, 159-173.